

The University of South Bohemia in České Budějovice, Faculty of Science

Diversity and distribution of particulate methane monooxygenase enzyme in known methanotrophic bacteria

Bachelor thesis

Student: **Palavinnage D. Sanchila Kumaranatunga**

Supervisor: **Dr. Anne Daebeler**

Consultant: **Vojtěch Tláškal, PhD**

České Budějovice, 2023

Kumaranatunga P.D.S., 2023: Diversity and distribution of particulate methane monooxygenase enzyme in known methanotrophic bacteria. Bc. Thesis, in English. – 31 p., Faculty of Science, University of South Bohemia, České Budějovice, Czech Republic.

Annotation:

A database of particulate methane monooxygenase enzyme in known methanotrophic bacteria was created and phylogenetic trees for the respective subunits making up this enzyme were created and analyzed.

Key words:

methanotrophs, particulate methane monooxygenase, subunit A, subunit B, subunit C, *pmoCAB*, *pxmABC*, operon, gene

Declaration:

I hereby declare that I have worked on my bachelor's thesis independently and used only the sources listed in the bibliography.

České Budějovice, 14th August 2023

.....
Palavinnage D. Sanchila Kumaranatunga

Abstract

Methanotrophs are bacteria capable of oxidizing methane to use it as both a carbon and energy source. This capability is due to the presence of the membrane integrated particulate methane monooxygenase (PMO) enzyme composed of three subunits: C, A and B. These subunits are arranged as operons in their genome, and potentially there is more than one operon in most methanotrophs. The orientation of the operons gives rise to two types of operons: the common *pmoCAB* found in most methanotrophs, and the rare *pxmABC* which is present in some microbial classes. This study aimed to understand the evolution of this enzyme. Phylogenetic trees were created for the three subunits based on their amino acid sequences and they were distinguished by their respective bacterial class. To create these phylogenetic trees, first a database was created with selected methanotrophs. The sequences were then downloaded from NCBI, they were aligned using MAFFT, processed through IQ-TREE and finally visualized using iTOL. The phylogenetic trees showed that the *pmoCAB* operons separated into different clades based on their microbial classes. Interestingly, the *pxmABC* operons were visualized in one separate clade which constituted of mainly *Gammaproteobacteria* and some *Alphaproteobacteria*. The presence of *pxmABC* in a significant number of *Alphaproteobacteria* is unique since there is little evidence of its presence in this class prior to this. Therefore, further studies of the presence of *pxmABC* genes in *Alphaproteobacteria* are required to fully understand its distribution in this microbial class.

Contents

Contents	iv
List of figures.....	v
1. Introduction.....	1
1.1. Methane and methanotrophs	1
1.2. Taxonomy of methanotrophs.....	2
1.3. Ecology of aerobic methanotrophs	2
1.4. Overall architecture, active site, and biochemistry of pMMO enzyme	3
1.5. The pMMO genome and operons	5
1.6. The pxm operon	6
1.7. Aims of the thesis	6
2. Materials and Methods.....	7
2.1. Creation of a database.....	7
2.2. R studio.....	7
2.3. Alignment and Phylogenetic trees.....	8
3. Results.....	9
3.1. Database of methanotrophs.....	9
3.2. Phylogenetic analysis.....	13
3.2.1. Phylogenetic analysis of subunit A	13
3.2.2. Phylogenetic analysis of subunit B	15
3.2.3. Phylogenetic analysis of subunit C	17
4. Discussion.....	21
4.1. Database.....	21
4.2. Phylogenetic trees	21
5. Conclusion	25
Bibliography	26

List of figures

Figure 1: Crystal structure of particulate methane monooxygenase enzyme in <i>Methylococcus</i> str. Bath (Lieberman & Rosenzweig, 2004b)	4
Figure 2 Methane oxidation pathways in methanotrophs (Hanson & Hanson, 1996).....	5
Figure 3 The length of the gene for the A subunit in five bacterial classes are shown with comparison between the two types of operons: pmo and pxm.	9
Figure 4 The length of gene of the B subunit in five bacterial classes are shown with comparison between the two types of operons: pmo and pxm.	11
Figure 5 The length of the gene of C subunit in five bacterial classes are shown with comparison between the two types of operons: pmo and pxm.	12
Figure 6 Maximum likelihood phylogenetic tree of subunit A amino acid sequences without precise branch lengths. The bacterial taxonomic classification is shown by the different branch colors. The type of operon is depicted by the highlights around the unique identifiers. Bootstrap values of branches that are only between 95 to 100% range are displayed as circles on the branches. The size of each circle corresponds to the bootstrap value.....	13
Figure 7 Maximum likelihood phylogenetic tree of subunit A amino acid sequences without precise branch lengths. The bacterial taxonomic classification is shown by the different branch colors. The type of operon is depicted by the highlights around the unique identifiers.	14
Figure 8 Maximum likelihood phylogenetic tree of subunit B amino acid sequences without precise branch lengths. The bacterial taxonomic classification is shown by the different branch colors. The type of operon is depicted by the highlights around the unique identifiers. Bootstrap values of branches that are only between 95 to 100% range are displayed as circles on the branches. The size of each circle corresponds to the bootstrap value.	15
Figure 9 Maximum likelihood phylogenetic tree of subunit B amino acid sequences without precise branch lengths. The bacterial taxonomic classification is shown by the different branch colors. The type of operon is depicted by the highlights around the unique identifiers.	16
Figure 10 Maximum likelihood phylogenetic tree of subunit C amino acid sequences without precise branch lengths. The bacterial taxonomic classification is shown by the different branch	

colors. The type of operon is depicted by the highlights around the unique identifiers. Bootstrap values of branches that are only between 95 to 100% range are displayed as circles on the branches. The size of each circle corresponds to the bootstrap value..... 17

Figure 11 Maximum likelihood phylogenetic tree of subunit C amino acid sequences without precise branch lengths. The bacterial taxonomic classification is shown by the different branch colors. The type of operon is depicted by the highlights around the unique identifiers. 19

List of tables

Table 1 List of pxmABC operon containing bacteria with their respective NCBI accession ID's. 20

1. Introduction

1.1. Methane and methanotrophs

Methanotrophs are a unique group of bacteria that have the capability to oxidize methane and use this process as an energy source. Additionally, methanotrophs utilize methane or carbon dioxide as a carbon source. Methane oxidation capability in these bacteria is attributed to the presence of the methane monooxygenase (MMO) enzyme. There are two distinct types of methane monooxygenase enzymes: a) particulate methane monooxygenase (pMMO) and b) a soluble methane monooxygenase (sMMO) (Hanson & Hanson, 1996). This thesis focuses on the presence of particulate methane monooxygenase (pMMO) enzyme, a membrane-bound enzyme. This enzyme belongs to the copper membrane monooxygenase (CuMMO) enzyme family which also includes the ammonia monooxygenases (AMO) and a few short-chain alkane and alkene monooxygenases (Khadka et al., 2018). The pMMO enzyme catalyses the initial oxygenation step in methane oxidation to produce methanol, which is then ultimately converted to respective metabolites depending on the type of methanotroph (Hanson & Hanson, 1996). The AMO enzyme is structurally similar to the pMMO enzyme, but it oxidizes ammonia instead of methane and is present in the ecological guild “nitrifiers” (Khadka et al., 2018).

Methane is a greenhouse gas contributing to global warming (Intergovernmental Panel on Climate Change, 2023). It is the second most potent greenhouse gas after carbon dioxide and absorbs more infrared radiation in comparison with carbon dioxide (Lieberman & Rosenzweig, 2004). Methane is also a major component of natural gas; a non-renewable fuel and is used extensively for the industrial and chemical production of methanol (Guerrero-Cruz et al., 2021). A possible mitigation strategy for global warming, increasing energy demands and a sustainable method of methanol production would be to use methanotrophic bacteria instead. This is because they can perform many biochemical conversions at ambient temperatures and pressures (Guerrero-Cruz et al., 2021).

1.2. Taxonomy of methanotrophs

Historically, methanotrophic bacteria were divided into the two categories based on their physical characteristics, metabolic pathways, phylogenetic analysis of the 16S rRNA gene sequences etc. into Type I methanotrophs (from the class *Gammaproteobacteria*) and Type II methanotrophs (from the class *Alphaproteobacteria*) (Hanson & Hanson, 1996). Type I methanotrophs use the ribulose monophosphate (RuMP) pathway for carbon fixation and include the bacterial genera *Methylobacter*, *Methylococcus*, *Methylmicrobium* and *Methylomonas*. Type II methanotrophs use the serine cycle and include the bacterial genera *Methylocystis* and *Methylosinus* (Hanson & Hanson, 1996; Knief, 2015). A third group belonging to the bacterial phylum *Verrucomicrobia* was later discovered in extreme environments and is thought to have a novel form of methane oxidation system (Dunfield et al., 2007; Islam et al., 2008; Pol et al., 2007). Op den Camp et al., (2009) proposed that these verrucomicrobial strains lack intracytoplasmic membranes and carbon fixation occurs by the Calvin-Benson-Bassham cycle. Further, genes for pMMO were identified in the anaerobic bacterial genus *Methylomirabilia* (NC10 bacteria), which has the exotic ability to produce intracellular oxygen to oxidize methane under anoxic conditions (Peng et al., 2022).

1.3. Ecology of aerobic methanotrophs

The energy gained from methane oxidation is the highest when oxygen serves as a final electron acceptor. Populations of methanotrophs are commonly found to be in environments with an excess of oxygen and sufficient methane concentration such as soil-overlying water interfaces in rice paddies and peatlands (Oremland & Culbertson, 1992; Reim et al., 2012). Recent research shows that methanotrophs are also able to oxidize methane at trace concentrations present in the atmosphere (Bay et al., 2021). However, it was later discovered that some proteobacterial methanotrophs are also present in environments with extreme conditions such as thermal springs, thermal lakes etc. (Kolb & Horn, 2012). This indicates the possibility of aerobic methanotrophs being able to function under micro-oxic conditions as well (Guerrero-Cruz et al., 2021). Kits et al., (2015) further found that the gammaproteobacterial *Methylomonas dinitrificans* can utilize nitrate ions as an oxidant for respiration, hence providing a method of energy conservation during hypoxic

conditions. Furthermore, methane oxidation coupled to iron reduction was also identified as an alternative to aerobic methane oxidation by Zheng et al., (2020). Most methanotrophic isolates were found to be neutrophilic and mesophilic, with some species being moderately acidophilic, psychrophilic, alkaliphilic and thermophilic (Op den Camp et al., 2009). In contrast to the proteobacterial methanotrophs, the verrucomicrobial methanotrophs were found only in extreme environments. They were first isolated in a geothermal soil in Hell's Gate (Tikitere), New Zealand, an acidic hot spring in Kamchatka, Russia, and a mud pot in Solfatara volcano, Italy by Dunfield et al., (2007); Islam et al., (2008); Pol et al., (2007) respectively. To date, they have only been found in geothermal habitats. The most significant characteristic feature of these bacteria is their extreme acidophilic nature allowing them to grow below pH 1. Additionally, they are reported to be capable of growth at high temperatures of almost 65 °C (Op den Camp et al., 2009).

1.4. Overall architecture, active site, and biochemistry of pMMO enzyme

The pMMO enzyme is a transmembrane enzyme dependent on copper as a cofactor and is composed of the three subunits called PmoA (β), PmoB(α), and PmoC(γ) encoded by the genes: *pmoA*, *pmoB* and *pmoC*. In the functional enzyme, the subunits are arranged as a cylindrical trimer of three protomers: $\beta_3\alpha_3\gamma_3$, with stability provided by glutamic acid, aspartic acid, and arginine residues (Koo et al., 2022; Lieberman & Rosenzweig, 2005). One copy each of PmoA, PmoB and PmoC is known as a protomer and is 100kDa in size (Figure 1) (Culpepper & Rosenzweig, 2012). According to Lieberman & Rosenzweig, (2005), PmoA and PmoC are almost entirely integrated into the plasma membrane. The PmoA subunit has seven transmembrane helices while PmoC has five transmembrane helices. However, PmoB subunit has soluble regions and therefore it is not entirely embedded in the cell membrane in contrast to PmoA and PmoC. The soluble regions are a N-terminal and a C-terminal cupredoxin domain located in the periplasm (Culpepper & Rosenzweig, 2012).

The active site of this enzyme is controversial due to the limitations of purification of this enzyme from the cell membrane (Chan & Lee, 2019). Crystal structures of the pMMO enzyme show that each protomer has three copper binding sites, with two of them located in the PmoB subunit. This

indicates the possibility of the active site being in the PmoB subunit (Culpepper & Rosenzweig, 2012; Lieberman & Rosenzweig, 2005). However, Koo et al., (2022) presents that the active site of this enzyme is in the PmoC subunit due to an intact PmoC scaffold including the Cu_C and Cu_D ligands. In addition, Ro et al., (2018) states that the active site located in PmoB is stabilized by the directly adjacent pmoC subunit, and thereby indicating the importance of both subunits for enzyme activity. Mutations in metal centre of related enzyme hydrocarbon monooxygenase C subunit abolished all activity while mutation in hydrocarbon monooxygenase B subunit abolished activity partly (Liew et al., 2014) thus confirming importance of the subunit C metal centre. Furthermore, the pMMO enzyme present in the phylum Verrucomicrobia might have a completely different active site due to the extreme environmental conditions it exists in (Culpepper & Rosenzweig, 2012).

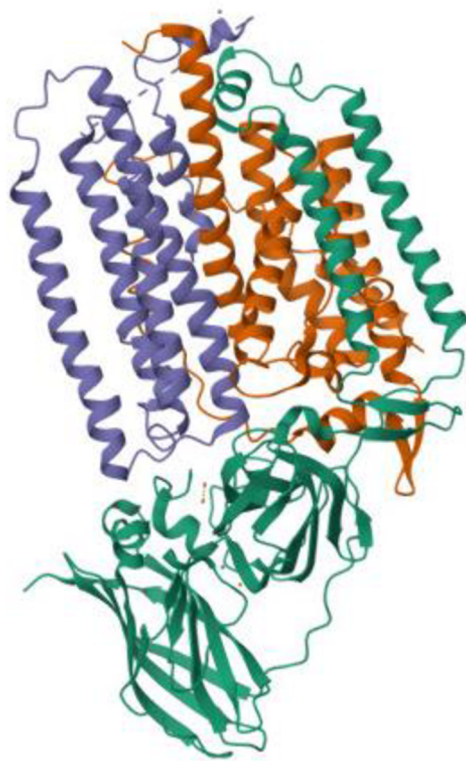


Figure 1: Crystal structure of particulate methane monooxygenase enzyme in Methylococcus str. Bath (Lieberman & Rosenzweig, 2004b)

The conversion of methane to methanol is the first step in methane oxidation. This step is catalysed by pMMO. Methanol is further converted to formaldehyde by methanol dehydrogenase

(Culpepper & Rosenzweig, 2012). Using these compounds, methanotrophs obtain carbon for cell material synthesis which is assimilated by different pathways depending on the type of methanotroph (Figure 2) (Hanson & Hanson, 1996; Op den Camp et al., 2009). However, pMMO lacks substrate specificity; in addition to methane, the enzyme also oxidises ammonia (Hanson & Hanson, 1996 and references therein).

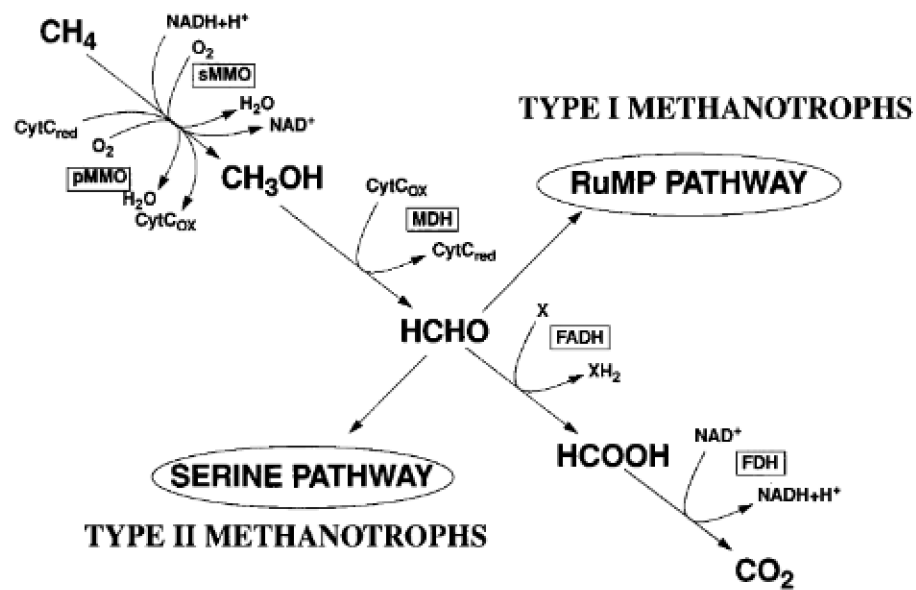


Figure 2 Methane oxidation pathways in methanotrophs (Hanson & Hanson, 1996)

1.5. The pMMO genome and operons

Due to the importance of the pMMO enzyme to sustain life of methanotrophs, the genes encoding for the pMMO subunits are overexpressed and therefore the enzyme represents approximately 20% of total cellular protein and in copper replete conditions it constitutes 80% of the total protein content in the cell membrane (Zhu et al., 2022 and references therein). The genes that code for the pMMO enzyme are organized in the gene order C-A-B which is known as the *pmoCAB* operon (Hanson & Hanson, 1996; Lieberman & Rosenzweig, 2004; Tavormina et al., 2011). Multiple *pmoCAB* operons within individual genomes are found to be present in both proteobacterial and verrucomicrobial methanotrophs. This occurrence is thought to have occurred due to gene

duplication events or as divergent copies with speculative evolutionary origins (Tavormina et al., 2011). It is possible, if a species possesses more than one *pmoCAB* operon in its genome, they would have different expression patterns, and the enzymes that it codes for have different methane affinities (Khadka et al., 2018 and references therein). In general, pMMO operons are transcriptionally activated by high levels of coppers, as copper is the main metal cofactor of pMMO (Chan & Lee, 2019).

1.6. The *pxm* operon

The *pxm* operon was first identified by Tavormina et al., (2011) in gammaproteobacterial methanotrophs. In contrast to the canonical *pmoCAB* operon, the *pxm* operon is organized in the gene order A-B-C and therefore termed as the *pxmABC* operon. This *pxmABC* operon also codes for three subunits, but its substrate specificity is yet unknown. In addition, it has been reported that gammaproteobacterial methanotrophs initially possessed the *pxmABC* operon only, but they later acquired the *pmoCAB* operon from an ancestor of the species *Nitrosococcus* and with time, most gammaproteobacterial methanotrophs have since lost the *pxmABC* operon (Khadka et al., 2018). The expression of the *pxmABC* operon occurs in hypoxic and nitrite rich conditions as reported by Kits et al., (2015) but the detailed regulation of this operon is not known.

1.7. Aims of the thesis.

1. To collect available DNA sequences of the subunit genes of particulate methane monooxygenase from cultivated methanotrophs and metagenome assembled genomes using public repositories.
2. To describe the diversity of particulate methane monooxygenase genes based on phylogenetic trees.
3. To study the occurrence of *pxmABC* genes in methanotrophs.

2. Materials and Methods

2.1. Creation of a database

The data for the database were retrieved from an existing database of known methanotrophic genomes, which were collected by colleagues in the Institute of Soil Biology and Biochemistry. In addition to this existing database, accession numbers of methanotrophs were retrieved from the NCBI using a list of methanotrophs published by Khadka et al., (2018). In addition to the accession ID's, genome metadata (source of isolation, contig number and length), number of operons, taxonomy etc. for each respective accession ID was identified in NCBI and stored in the database as well.

Afterwards, nucleotide sequences for each respective accession ID (for the three PMO subunits) were downloaded from NCBI (Sayers et al., 2022) and stored locally together with their accession ID as FASTA format. To obtain amino acid sequences, nucleotide sequences translated using EMBOSS Transeq available in EMBL-EBI (Madeira et al., 2022).

The link to the database is available at [10.5281/zenodo.8133669](https://doi.org/10.5281/zenodo.8133669)

2.2. R studio

The database was processed in R studio version R 4.2.2 (R Core Team, 2022). The R packages used includes ggplot2 (Hadley Wickham, 2016), dplyr (Hadley Wickham et al., 2022), openxlsx (Philipp Schaubberger & Alexander Walker, 2022), and readxl (Hadley Wickham & Jennifer Bryan, 2022). Using R studio, the average lengths, and standard deviations of individual subunits for each accession ID were calculated and visualized based on the position of the first and last nucleotide in genomes.

2.3. Alignment and Phylogenetic trees

The amino acid sequences of *pmoCAB* from isolates and metagenome assembled genomes (MAGs) were used as input into analysis. Genomes with ≥ 1 subunit missing in annotation were removed from subsequent analysis. Those taxa classified as ‘alkane oxidisers’, ‘alkene oxidisers’, and ‘unknown’ in NCBI, and not known for methanotrophic activity in literature were also removed (a total of 7 species from the database were excluded in further analysis). Additionally, ‘Archaea’ were also removed from further analysis (a total of 4 species were excluded in this category).

For each separate subunit, an alignment was done using amino acid sequences as input and the online MAFFT program with default settings: scoring matrix used was BLOSUM62, default guide tree, UniRef50 (Kato et al., 2018). Afterwards, the aligned sequences were used to construct maximum likelihood trees using IQ-TREE (Nguyen et al., 2015; Trifinopoulos et al., 2016). The best fit model LG+G4, LG+F+I+G4, and LG+I+G4 respectively for PmoA, PmoB and PmoC was found by Model Finder (Kalyaanamoorthy et al., 2017), and the trees were calculated with 1000 bootstraps iterations (Minh et al., 2013). Finally, to visualize the phylogenetic tree, iTOL was used (Letunic & Bork, 2021) with iTOL annotation editor v1.7. In all cases, trees were calculated as unrooted and as rooted, with sequences of AmoA, AmoB, and AmoC of nitrifiers from *Betaproteobacteria* serving as the outgroup. Branch lengths are displayed for unrooted trees while for rooted circular trees, the distances of individual groups are omitted.

3. Results

3.1. Database of methanotrophs

A total of 112 genomes from 8 different microbial classes were procured from an existing database of known methanotrophic genomes, which were collected by colleagues in the Institute of Soil Biology and Biochemistry and from Khadka et al., (2018). The database consisted of a total of 182 operons for these 112 genomes (mean of 1.6 operon per genome), while all three subunits were available for 167 operons from 102 of those genomes. All operons were allocated a unique identifier. This was based on the genome and the operon numbering system from the database. Isolation source characteristics were available only for 51% of the genomes. In addition, 75 genomes (67% from the total genomes) contained ≤ 3 contigs including plasmids and thus represented near-complete genomes. 44 (26% of the total operons) were metagenome assembled genomes (contig number ≥ 16) with an average contig number of 181 ± 238 .

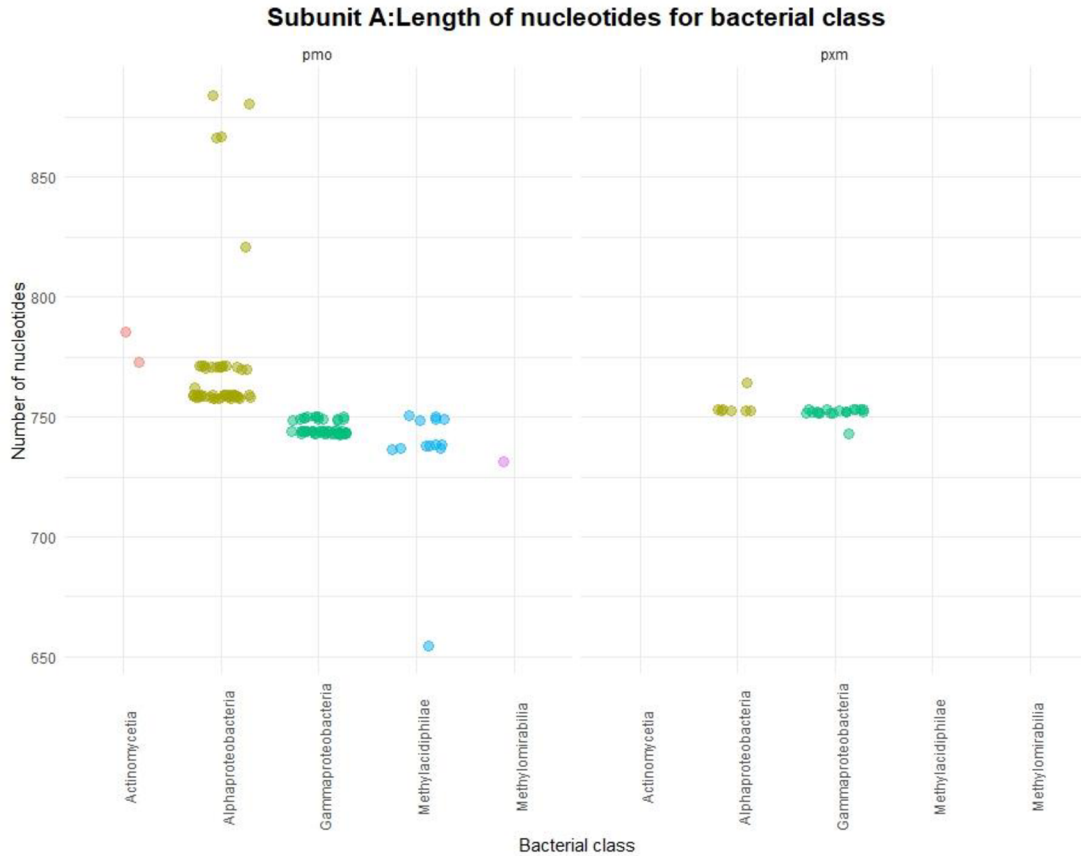


Figure 3 The length of the gene for the A subunit in five bacterial classes are shown with comparison between the two types of operons: *pmo* and *pxm*.

The database also included the start and stop nucleotide positions for each subunit and number of nucleotides for each subunit per operon. Figure 3 shows the average length of the gene sequence for subunit A in each bacterial class, but it also shows the difference of the length of this subunit with respect to the two types of operons: *pmo* and *pxm*.

The *pxm* gene was only found to be present in the bacterial classes *Gammaproteobacteria* and *Alphaproteobacteria* and the average length was 753 ± 3 nucleotides. The overall average length of the *pmoA* gene in all bacterial classes was found to be 756 ± 27.4 nucleotides. However, on average, the longest *pmoA* gene were present in the bacterial class- *Actinomycetia* with a length of 779 ± 8.49 nucleotides long and on average the shortest *pmoA* gene was present in *Methylomirabilia* which have an average length of 731 ± 0 nucleotides.

Figure 4 shows the average gene length of the B subunit in each bacterial class, with comparison between the two types of operons: *pmo* and *pxm*. The average length of the *pxmB* operon was 1239 ± 15.7 nucleotides while the average length of the *pmo* operon was 1258 ± 28.7 nucleotides. Similar to subunit A, the longest average length of *pmoB* operon was found in *Alphaproteobacteria* and *Methylacidphilae* with 1272 ± 22.9 nucleotides and 1272 ± 24.0 nucleotides respectively. The shortest average length was found in *Gammaproteobacteria* with 1241 ± 25.9 nucleotides. The average nucleotides length of subunit B is the highest from all three subunits. Again, the *pxmB* gene was found only in the two classes *Alpha-* and *Gammaproteobacteria*.

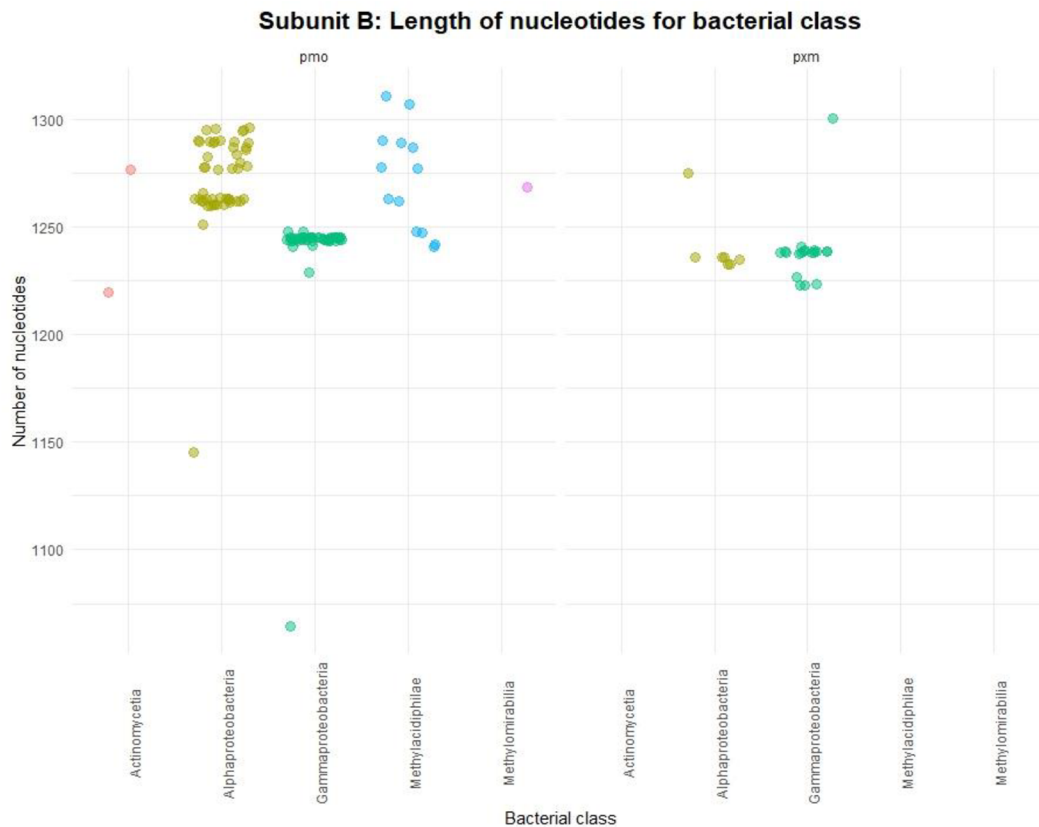


Figure 4 The length of gene of the B subunit in five bacterial classes are shown with comparison between the two types of operons: *pmo* and *pxm*.

Figure 5 shows the average length of *pmo* and *pxm* genes in five bacterial classes with respect to subunit C. The average length of the *pxmC* gene was found to be 774 ± 2.76 nucleotides, while the average length of the *pmoC* gene is 777 ± 38.4 nucleotides. This difference in average length between the *pmoC* and *pxmC* showed the least difference of all three subunits. In contrast to subunits A and B, the longest average length of the *pmoC* operon was found to be 875 ± 17.0 nucleotides in the bacterial class- *Actinomycetia* while the shortest average length was found in *Gammaproteobacteria* with 763 ± 35.9 nucleotides on average.

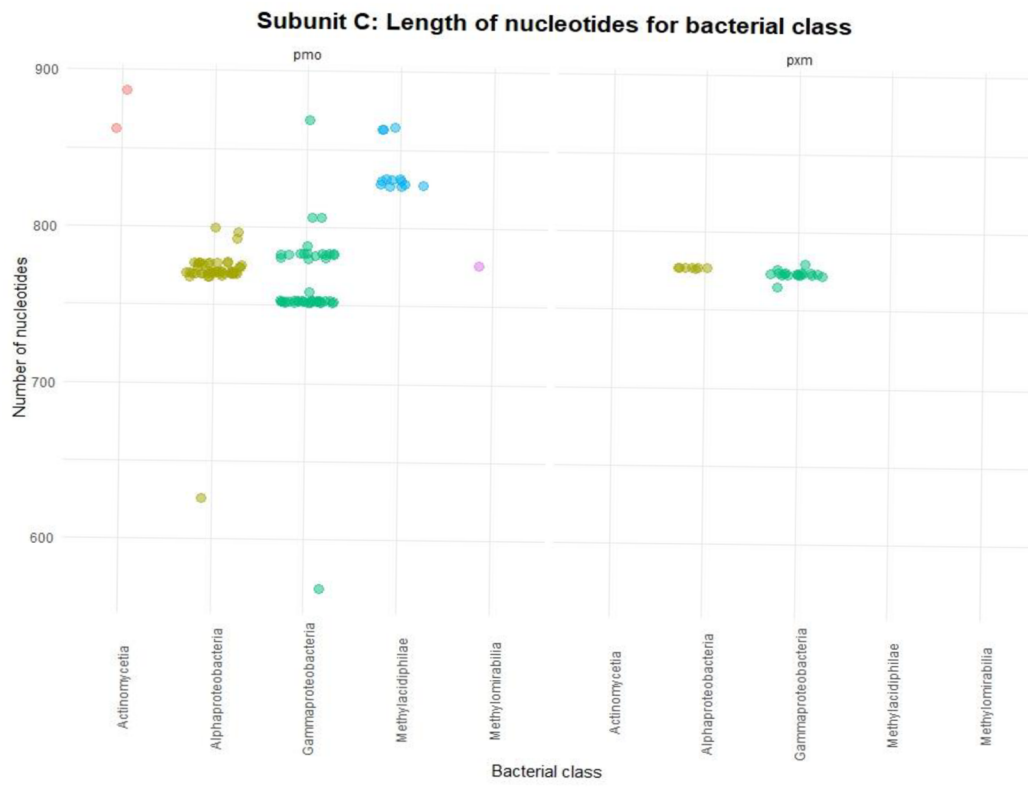


Figure 5 The length of the gene of C subunit in five bacterial classes are shown with comparison between the two types of operons: pmo and pxm.

3.2. Phylogenetic analysis

3.2.1. Phylogenetic analysis of subunit A

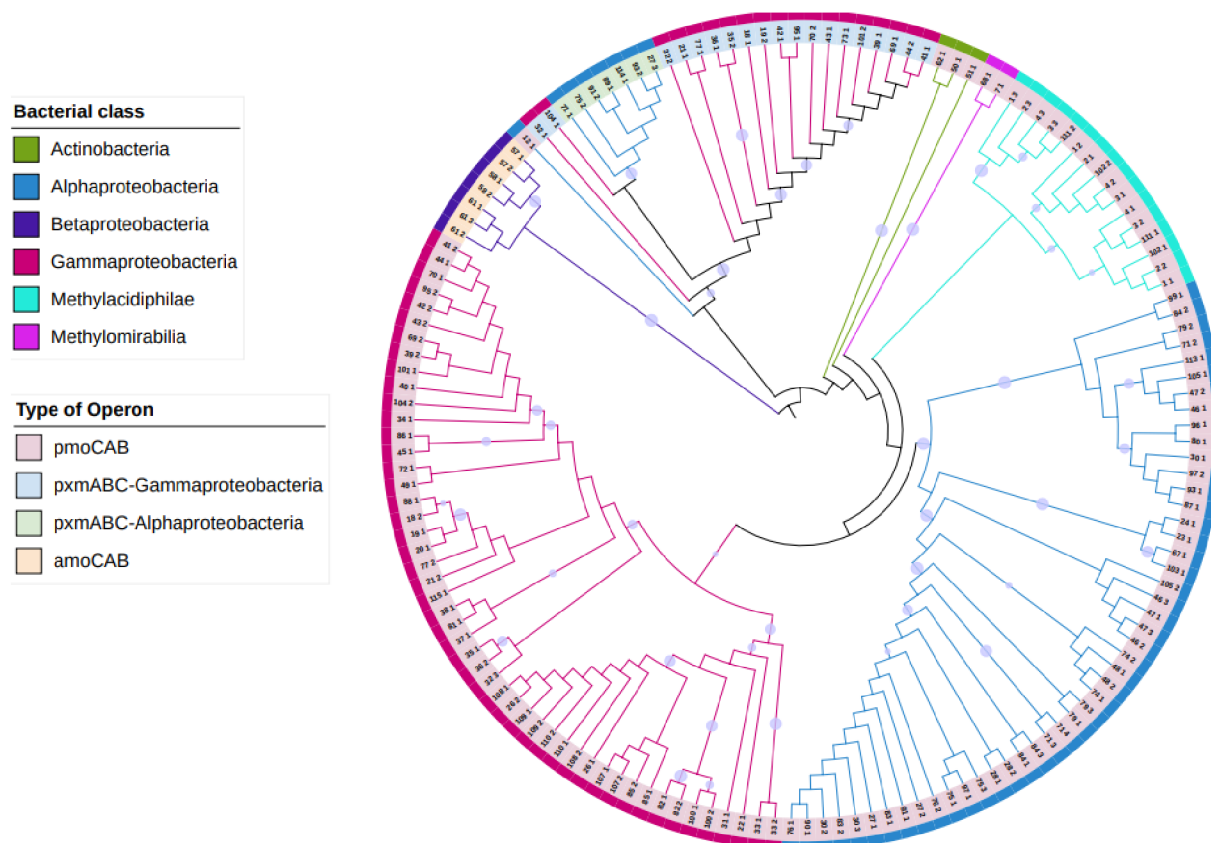


Figure 6 Maximum likelihood phylogenetic tree of subunit A amino acid sequences without precise branch lengths. The bacterial taxonomic classification is shown by the different branch colors. The type of operon is depicted by the highlights around the unique identifiers. Bootstrap values of branches that are only between 95 to 100% range are displayed as circles on the branches. The size of each circle corresponds to the bootstrap value.

To describe the diversity of the methane monooxygenase enzyme, phylogenetic trees for individual subunits were constructed. A total of 152 amino acid sequences were used to create the phylogenetic tree of subunit A (Figure 6 & 7). The *pmoCAB* operon represents 78.1% of all operons in the dataset and therefore, is the most common type of operon. In contrast, the *pxmABC* operon represents only a total of 17.1% of which 12.5% is from *Gammaproteobacteria* and only 4.6% from the *Alphaproteobacteria*. The remaining operons (4.6%) is the *amoCAB* from the

'betaproteobacterial ammonia-oxidisers'. As figures 6 and 7 show, the *pmoA* genes cluster together corresponding to bacterial taxonomy. In contrast, the *pxmA* genes all fell into a separate polyphyletic cluster with both bacterial classes: *Gammaproteobacteria* and *Alphaproteobacteria*, together. Interestingly, the polyphyletic cluster also contained a single *pmoA* gene (ID:12_1) belonging to *Alphaproteobacteria* as well.

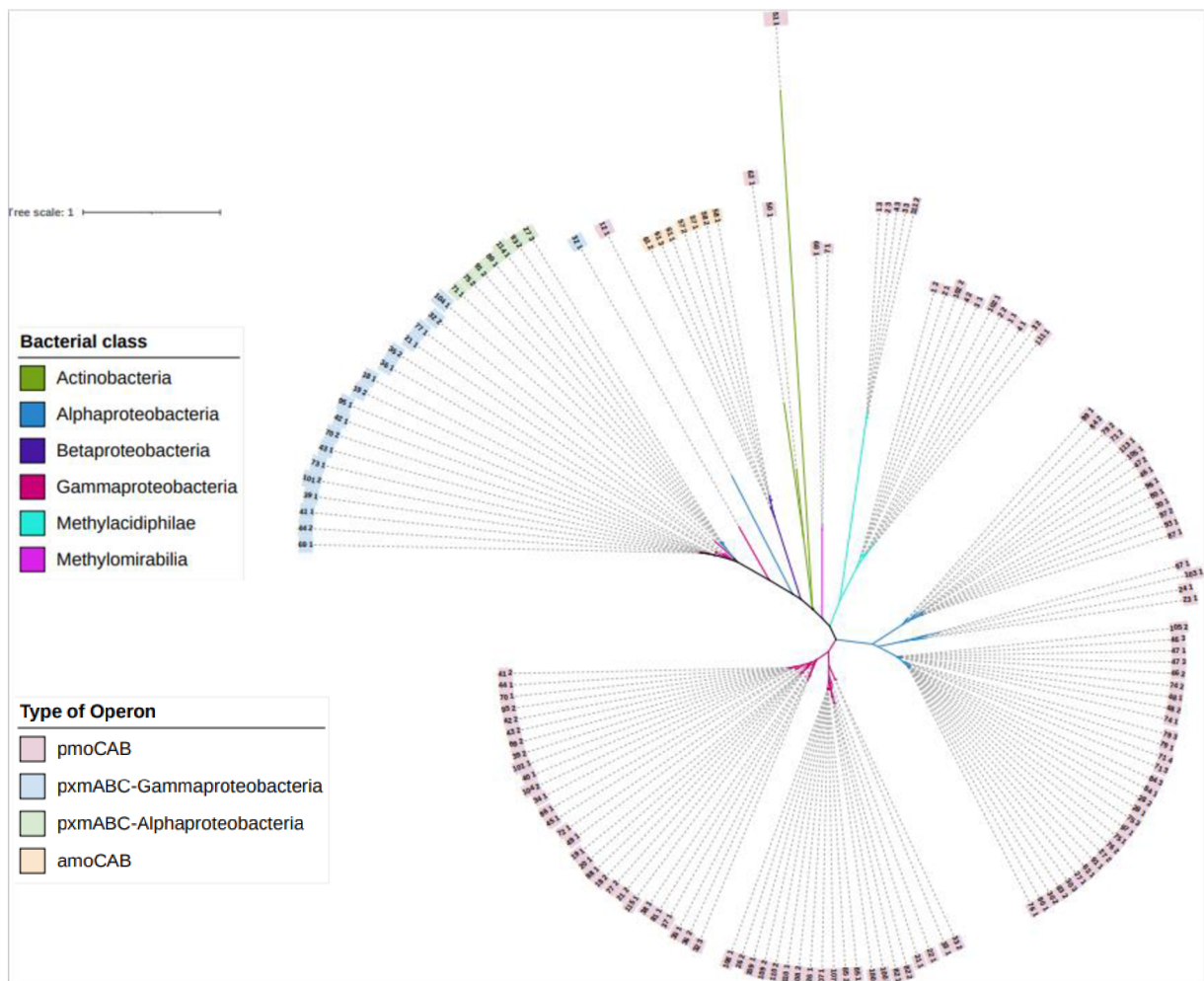


Figure 7 Maximum likelihood phylogenetic tree of subunit A amino acid sequences without precise branch lengths. The bacterial taxonomic classification is shown by the different branch colors. The type of operon is depicted by the highlights around the unique identifiers.

3.2.2. Phylogenetic analysis of subunit B

A total of 150 genes from the database were used to create the phylogenetic tree of subunit B. Most of these were the *pmoB* operon, representing 77.3%. In contrast, *pxmB* gene represented 17.4% of all B subunits of which the majority belongs to the *Gammaproteobacteria* (12.7%) and the rest to *Alphaproteobacteria* (4.7%). The remaining 5.3% belonged to the betaproteobacterial ammonia-oxidisers (Figure 8 and 9). The *pmoB* genes clustered into separate monophyletic branches according to the bacterial class. However, the *pxmB* genes fell into one branch from all *pmoB* genes, and this branch consisted of both bacterial classes: *Gammaproteobacteria* and *Alphaproteobacteria*. Interestingly, the outgroup contained a singular *pmoB* gene (ID: 12_1) belonging to *Alphaproteobacteria*.

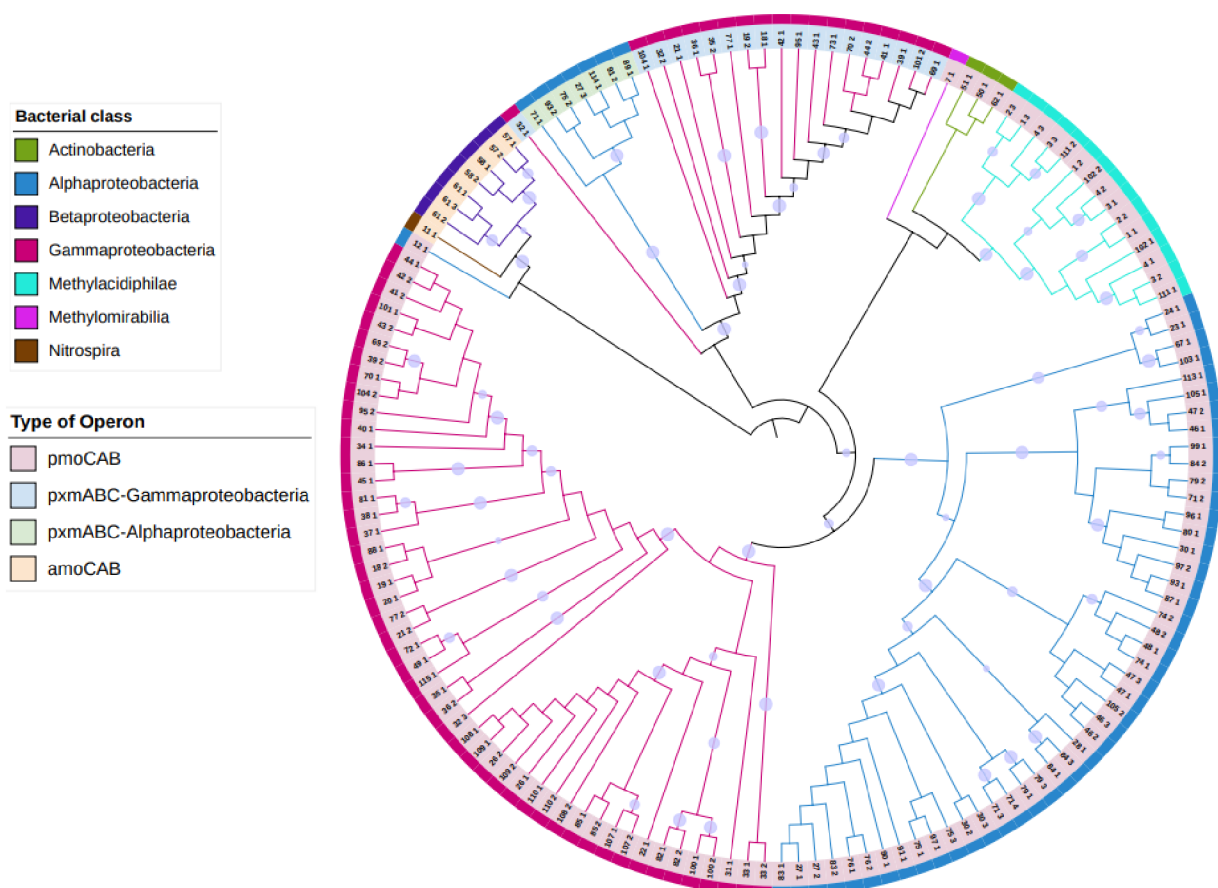


Figure 8 Maximum likelihood phylogenetic tree of subunit B amino acid sequences without precise branch lengths. The bacterial taxonomic classification is shown by the different branch colors. The type of operon is depicted by the highlights around the unique identifiers. Bootstrap values of branches that are only between 95 to 100% range are displayed as circles on the branches. The size of each circle corresponds to the bootstrap value.

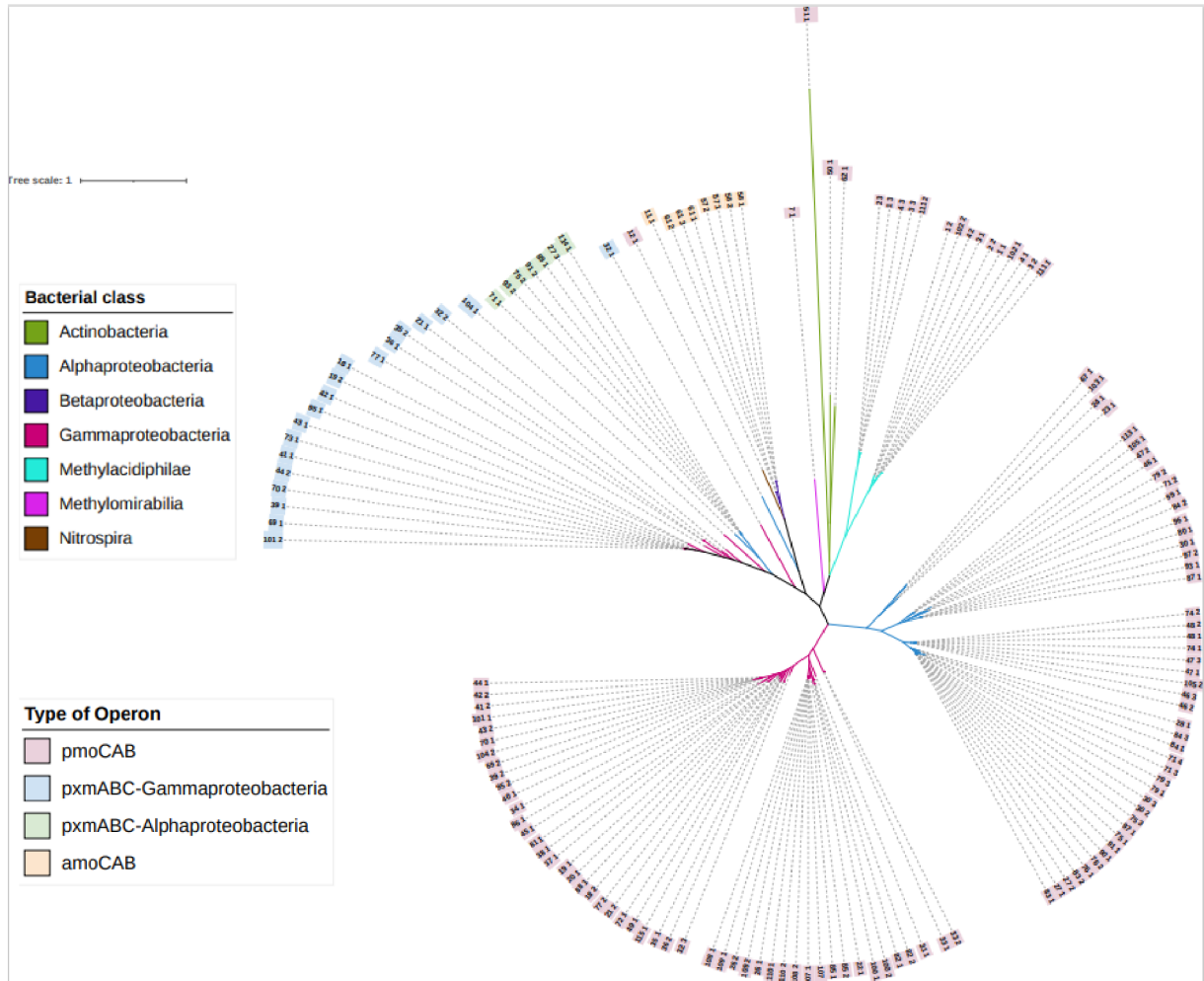


Figure 9 Maximum likelihood phylogenetic tree of subunit B amino acid sequences without precise branch lengths. The bacterial taxonomic classification is shown by the different branch colors. The type of operon is depicted by the highlights around the unique identifiers.

3.2.3. Phylogenetic analysis of subunit C

A total of 152 genes from the database were used to create the phylogenetic tree for subunit C (Figures 10 & 11). 77.6% of these 152 genes were the *pmoC* genes. These *pmoC* genes formed separate branches according to the bacterial class they affiliate with. The *pxmC* genes represented 17.1% of the total subunit C genes, of which the majority belonged to *Gammaproteobacteria* (12.5%) and the remainder to *Alphaproteobacteria* (4.6%). Both trees (Figure 10 & 11) show that the *pmoC* gene formed separate monophyletic branches reflecting their affiliation with bacterial class. All *pxmC* genes fell into a separate cluster from the *pmoC* genes, but the grouping was polyphyletic with respect to the two different bacterial classes: *Gammaproteobacteria* and *Alphaproteobacteria*. Interestingly, the outgroup contained a singular *pmoC* gene (ID: 12_1) belonging to *Alphaproteobacteria*.

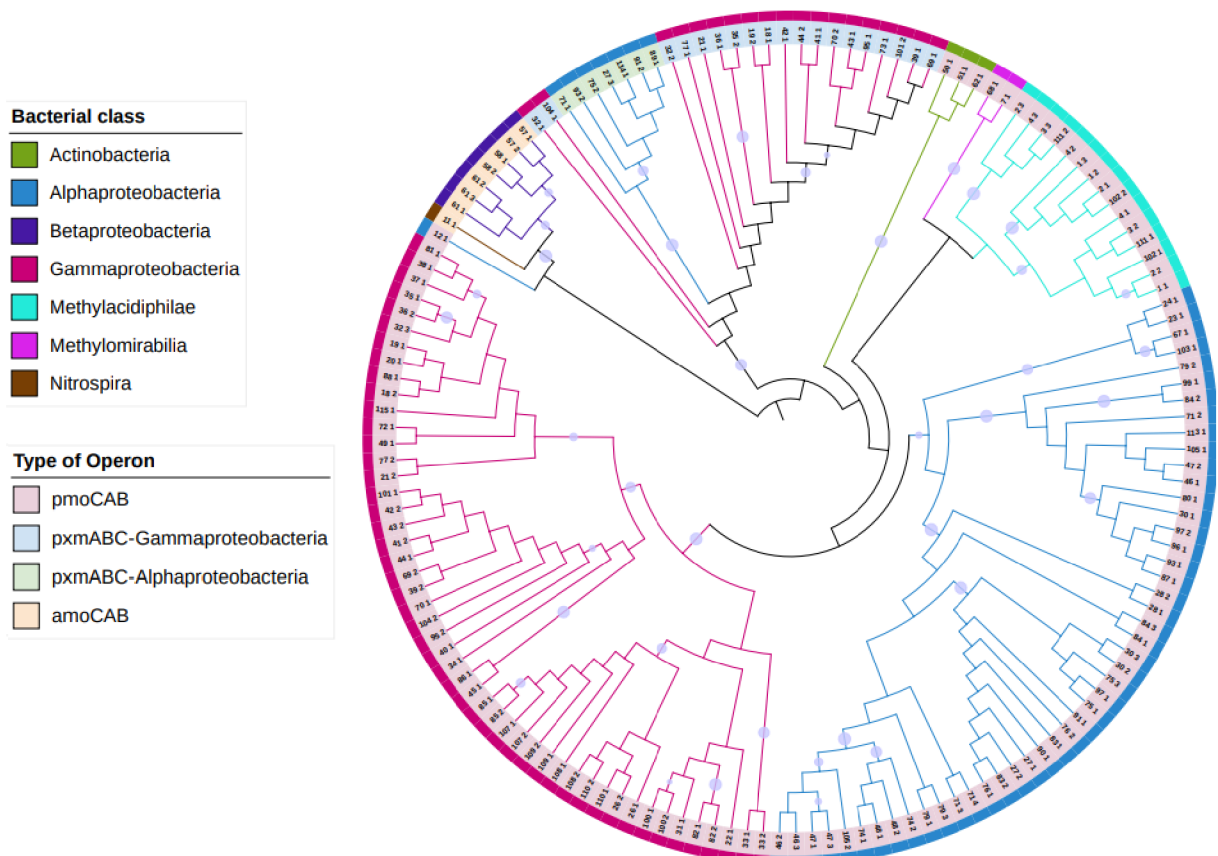


Figure 10 Maximum likelihood phylogenetic tree of subunit C amino acid sequences without precise branch lengths. The bacterial taxonomic classification is shown by the different branch colors. The type of operon is depicted by the highlights around the unique identifiers. Bootstrap values of branches that are only between 95 to 100% range are displayed as circles on the branches. The size of each circle corresponds to the bootstrap value.

The branching of the three subunits with respect to bacterial classes were similar in all three phylogenetic trees. The *pmoCAB* operon was present in nearly all species, except for *Methylomonas koyamae* strain LM6 (ID: 73_1, bacterial class: *Gammaproteobacteria*, bacterial genus: *Methylomonas*), *Methylocystis* sp. H15 MCYSTISH15_contig0030 (ID: 89_1, bacterial class: *Alphaproteobacteria*, bacterial genus: *Methylocystis*), and *Methylocystis* sp. SB2 (ID: 114_1, bacterial class: *Alphaproteobacteria*, bacterial genus: *Methylocystis*) which only contained a *pxmABC* operon.

The *pxmABC* operon was present only in the bacterial classes *Gammaproteobacteria* and *Alphaproteobacteria*. The gammaproteobacterial genera that contained this *pxmABC* operon were *Methylobacter*, *Methyloglobulus*, *Methylmicrobium*, *Methylomonas*, and *Methylococcus*. The alphaproteobacterial *pxmABC* operon was present only in the *Methylocystis* genus (Table 1).

The highest number of operons present in a single species, regardless of the type of operon, was found in the complete genome of *Methylocystis bryophila* strain S285 (*Alphaproteobacteria*, ID 71, RefSeq accession GCF 002117405.1) with four operons. Three of these operons were the more common *pmoCAB* operon and the remaining, a *pxmABC* operon.

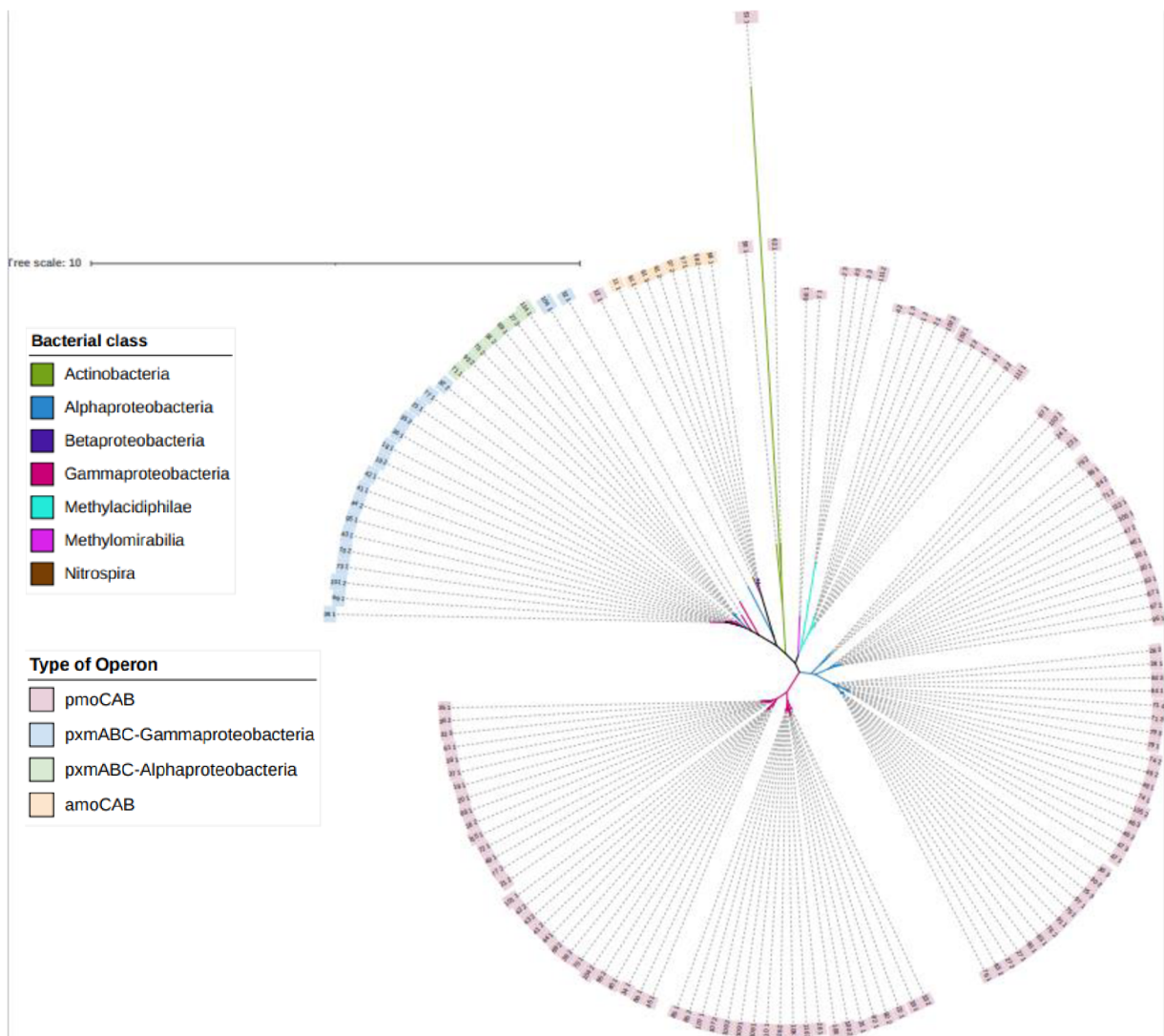


Figure 11 Maximum likelihood phylogenetic tree of subunit C amino acid sequences without precise branch lengths. The bacterial taxonomic classification is shown by the different branch colors. The type of operon is depicted by the highlights around the unique identifiers.

Genome	NCBI Accession ID	Subunit A Accession ID	Subunit B Accession ID	Subunit C Accession ID
Methylobacter luteus IMV-B-3098	1095552	WP_027157616	WP_027157617	WP_027157618
Methylobacter marinus A45	674036	WP_020159526	WP_020159527	WP_027147300
Methylobacter tundripaludum SV96	697282	EGW22253	EGW22254	EGW22255
Methylocystis rosea SV97	1132444	WP_198008876	WP_018409560	WP_018409559
Methyloglobulus morosus KoM1	1116472	MKO_MKO1_c77.74	MKO_MKO1_c77.74	MKO_MKO1_c77.74
Methyloglobulus morosus KoM1	1116472	MKO_MKO1_c123.115	MKO_MKO1_c123.115	MKO_MKO1_c123.115
Methylomicrobium agile ATCC35068	39774	CC94DRAFT_2805	CC94DRAFT_2804	CC94DRAFT_2803
Methylomicrobium album BG8	686340	EIC29218	EIC29219	EIC29217
Methylomonas koyamae JCM 16701	1294261	Ga0128345_10382	Ga0128345_10383	Ga0128345_10381
Methylomonas sp. 11b	1168169	Meth11bDRAFT_3086	Meth11bDRAFT_3087	Meth11bDRAFT_3088
Methylomonas sp. FJG1	1538553	JTDD01000035	JTDD01000035	JTDD01000035
Methylomonas sp. LW13	107637	U737DRAFT_scaffold00022.22	U737DRAFT_scaffold00022.22	U737DRAFT_scaffold00008.8
Methylomonas sp. MK1	1131552	G006DRAFT_scaffold00001.1	G006DRAFT_scaffold00001.1	G006DRAFT_scaffold00001.1
Methylomonas sp. DH-1	1727196	ANE56981.1	ANE56982.1	ANE56983.1
Methylomonas sp. LWB	1905845	OHX34473.1	OHX34472.1	OHX34471.1
Methylocystis bryophila strain S285	655015	ARN79806.1	ARN79805.1	ARN79804.1
Methylomonas koyamae strain LM6	702114	ATG91943.1	ATG91944.1	ATG91945.1
Methylocystis hirsuta strain CSC1 Contig1	369798	RNJ51621.1	RNJ49446.1	RNJ49445.1
Candidatus Methylobacter oryzae strain KRF1 C943	2497749	TRW92170.1	TRW92169.1	TRW92216.1
Methylocystis sp. H15 MCYSTISH15_contig0030	2785787	MBG0806172.1	MBG0806173.1	MBG0806174.1
Methylocystis sp. L43 MCYSTISL43_contig0019	2785790	MBG0796885.1	MBG0796886.1	MBG0796887.1
Methylocystis sp. H4A MCYSTISH4A_contig0001	2785788	MBG0803417.1	MBG0803416.1	MBG0803415.1
Methylomonas sp. LL1	2785785	QPK63628.1	QPK63627.1	QPK63626.1
Methylomonas sp. EFPC1	2812648	QSB01236.1	QSB01235.1	QSB01234.1
Methylomonas paludis strain S2AM	1173101	QWF71931.1	QWF71932.1	QWF71933.1
Methylocystis sp. SB2	743836	ULO23796.1	ULO23795.1	ULO23794.1

Table 1 List of *pxmABC* operon containing bacteria with their respective NCBI accession ID's.

4. Discussion

4.1. Database

Methanotrophs are well studied due to their contribution to mitigating methane emissions via the production of methane monooxygenase, an enzyme of the CuMMO family. The database that was created for this thesis was on the particulate methane monooxygenase which has two types encoded by two different operons: the canonical *pmo* operon where the subunits are arranged in C-A-B order and the rarer *p_{xm}* operon where the subunit arrangement is A-B-C (Hanson & Hanson, 1996; Tavormina et al., 2011).

In this thesis, subunit C shows the most conservation from all the three subunits. However, *Gammaproteobacteria* shows the least conservation in subunit C while it shows significant conservation in subunits A and B. Interestingly, *Methylophilae* shows only slightly varying lengths in all three subunits, with the most conservation observed in subunit C with a standard deviation of 15 nucleotides. Furthermore, lengths in certain taxonomic groups display subclass grouping which might be caused by conserved lengths at lower levels of bacterial taxonomy. Thus, two populations of subunit lengths are visible in the case of subunit C of *Gammaproteobacteria* (Figure 5) and subunits A and B of *Alphaproteobacteria* (Figures 3 & 4). According to a study done by Sharir-Ivry & Xia, (2021), it is assumed that catalytic sites of proteins show a strong degree of conservation. Based on these results, this might support the possibility of the active site of this enzyme being present in subunit C (Koo et al., 2022). In addition, it is known that membrane proteins are less conserved than cytoplasmic proteins (Sojo et al., 2016). However, though the PMO enzyme is an integral membrane protein, the significant conservation across all three subunits shows the importance of this enzyme for the sustenance in methanotrophs.

4.2. Phylogenetic trees

To examine evolutionary relationships and history, phylogenetic trees were constructed. In this study, nucleotide sequences for all subunits of the PMO enzyme were translated into amino acid sequences, and these were then used to construct phylogenetic trees.

In general, the phylogenetic trees of all three subunits had a similar pattern as shown by Figures 6-11. This could indicate that all three subunits have almost the same evolutionary history and are passed down through generations as a unified operon as supported by Khadka et al., (2018). The unrooted phylogenetic trees of all three subunits shows that there are three major branches. The first branch was made up of alphaproteobacterial methanotrophs and the second branch contained *Gammaproteobacteria*. The final major branch contained the betaproteobacterial AMO subunits, the actinobacterial and the verrucomicrobial *pmoCAB* operons and finally the *pxmABC* operons. This topology is similar to one of the phylogenetic trees constructed by Tavormina et al., (2011). However, this study also considered the *pxmABC* operons from *Alphaproteobacteria*, which were first reported by Khadka et al., (2018) in two species belonging to the bacterial genus *Methylocystis*. This study has found a total of 7 species to contain the *pxmABC* operon, all of which belong to *Methylocystis* too. However, not all *Methylocystis* species investigated in this study had a *pxmABC* operon, for example, *Methylocystis sp. Rockwell ATCC49242* (ID: 28) and *Methylocystis rosea strain GW6* (ID: 76) has only two *pmoCAB* operons while *Methylocystis sp. SC2* (ID: 30) has only three *pmoCAB* operons.

The branch containing the *pxmABC* operons is also observed closer to the branch with nitrifiers: the *Betaproteobacteria*. Due to the occurrence of the *pxm* operon in nature, it has not been studied deeply and the function of the enzyme it codes for is largely speculative. However, its clustering next to nitrifiers in the phylogenetic analysis of this thesis could indicate that the *pxmABC* operon produces a variation of the monooxygenase enzyme, that has the capability to oxidise ammonia, methane or even for detoxification (Tavormina et al., 2011). In the case of *Methylomicrobium album*, it has two operons: a *pmoCAB* operon (ID 36_2) and a *pxmABC* operon (ID 36_1). The *pxmABC* operon in this species has been found to be capable of ammonia-oxidation (Tavormina et al., 2011). Additionally, it has been speculated that the expression of the *pxm* operon depends on environmental conditions such as exposure to ammonia (Tavormina et al., 2011). Furthermore, *Methylocystis sp. SB2* (ID 114_1) was first isolated by Im et al., (2011) and was reported to grow in methane, acetate as well as ethanol. In the work done for this thesis, this species was found to have the *pxmABC* operon and this strongly hints at the possibility that the enzyme encoded by this operon can oxidise methane, acetate, as well as ethanol (Im et al., 2011).

The *Methylacidiphilae* belong to the phylum *Verrucomicrobia*. In this study, it was found that these bacteria possess only the *pmoCAB* operon. In addition, it can be observed in the phylogenetic trees (Figures 6 to 11) that the *Verrucomicrobia* share a close relation with *Proteobacteria*. According to Dunfield et al., (2007) and Op den Camp et al., (2009) this is a possible indication of an ancient divergence of the two phyla rather than a recent lateral gene transfer of the *pmoCAB* operon and these bacteria possibly show no growth in the absence of methane as reported by Islam et al., (2008) from their isolation of the bacterium *Methylacidiphilum kamchatkense*.

This study also includes the *Actinobacteria*: *Mycobacterium chubuense* NBB4 (ID: 50_1), *Mycobacterium rhodesiae* NBB3 (ID: 51_1), and *Nocardioideae* bacterium *Broad-1* (ID: 62_1). NCBI has annotated these organisms as methanotrophs, and they are said to contain the pMMO enzyme. The phylogenetic trees show that the *pmo* genes in these bacteria are quite possibly closely related to those of betaproteobacterial ammonia oxidisers and to those of *Verrucomicrobia*. However, the analysed operon from *Mycobacterium rhodesiae* NBB3 (ID 51_1) is possibly an outlier in the alignment and probably codes for an enzyme with a function other than methane oxidation. In addition, another operon from this species released only recently, is again annotated in NCBI as *pmoCAB* and has potentially higher similarity to the classical *pmo*. Methanotrophy in *Actinobacteria* has been discovered by van Spanning et al., (2022) in the bacterial genus *Mycobacterium*. These *Actinobacteria* were isolated from a highly acidic biofilm in a cave in Romania. They were identified to be methanotrophs due to the presence of soluble methane monooxygenase (sMMO), but not pMMO, as well as their ability to utilize methane as a sole carbon source via the RuMP pathway. The presence of *pmoCAB* in the phylum of *Actinobacteria* detected in this thesis should be taken with caution as its function needs to be described by in vitro experiments.

Bradyrhizobium sp. *ERR11* (ID:12_1) was observed in the outgroup (containing *Betaproteobacteria*) in the phylogenetic trees of subunits B and C (Figures 8 to 11) but in the phylogenetic tree of subunit A (Figures 6 and 7) it was observed in the polyphyletic cluster containing the *pxmA* gene. *Bradyrhizobium* is known to fix nitrogen and can be detected together with methanotrophs (Cui et al., 2022). This could be the reason of its presence in the outgroup of

subunit B and C phylogenetic trees. In addition, the close relationship between the *Bradyrhizobium* and the polyphyletic cluster containing the *pxmA* gene in subunit A supports the ability of *pxmA* gene to be involved in nitrogen fixation (Kits et al., 2015).

Most of the bacterial species analysed in this study were shown to have multiple operons with *Methylocystis bryophila* strain S285 (ID: 71, bacterial class: *Alphaproteobacteria*, bacterial genus: *Methylocystis*) having a total of four operons, one of which is a *pxmABC* operon. This species is suggested to be well adjusted to growth in peatlands due to possession of two methane-oxidising isoenzymes: a pMMO with low-affinity and a pMMO with high affinity (Han et al., 2018). However, this affinity of the two enzymes needs to be verified by in-vitro experiments. Generally, most methanotrophs have multiple copies of *pmoCAB* operons. However, some species have one or more *pmoCAB* operon and the *pxmABC* operon as well. The presence of multiple copies is thought to be due to gene duplication events or as divergent copies with speculative evolutionary origins due to different environmental conditions (Tavormina et al., 2011). Furthermore, it was described in this study that three species had only the *pxmABC* operon: *Methylomonas koyamae* strain LM6 (ID 73_1), *Methylocystis* sp. H15 MCYSTISH15_contig0030 (ID 89_1), and *Methylocystis* sp. SB2 (ID 114_1). However, *pmoCAB* operons have been sequenced in *Methylocystis* sp. H15, *Methylomonas koyamae* LM6, and *Methylocystis* sp. SB2 by de Assis Costa et al., (2021); Lee et al., (2020); Vorobev et al., (2014) respectively. The *Methylocystis* sp. H15, also contained the soluble methane monooxygenase enzyme as well (de Assis Costa et al., 2021) but this was not reported in the other two species. Interestingly, *Methyloglobulus morosus* KoM1 (ID: 31) was found to be the only species in our database that contained two *pxmABC* operons with one *pmoCAB* operon. This species is known to grow on methane, but also can fix nitrogen as well (Deutzmann et al., 2014).

5. Conclusion

The aim of this study was to create a database of known methanotrophs and their particulate methane monooxygenase (pMMO) enzyme that is responsible for their ability to oxidise methane which is an important ecological trait. This enzyme is made up of three subunits; subunits A, B and C, which are genetically encoded by their respective genes; A, B and C. Methanotrophs have two types of operons a) the common *pmoCAB* operon and b) the rare *pxmABC* operon. Using amino acid sequences of the two different sets of *pMMO* genes collected into the database, phylogenetic trees were created to be able to study their evolutionary relationships. The final aim was to study the occurrence of the *pxmABC* operon in methanotrophs. The phylogenetic trees of the three subunits showed that they were significantly similar, thereby allowing us to substantially assume that this operon is transferred through the generations as a unified operon. All three phylogenetic trees had three major branches: one branch with *pmoCAB* operons from *Gammaproteobacteria*, second branch with *pmoCAB* operons from *Alphaproteobacteria* and the final branch with the *Betaproteobacteria*, the *Actinobacteria*, the *Verrucomicrobia* and *pxmABC* operons belonging to *Gammaproteobacteria* and *Alphaproteobacteria*. Remarkably, this study found a significant number of *pxmABC* operons belonging to *Alphaproteobacteria* and it is increasingly significant that this rarer type of operon has different functions, but they are yet to be conclusively recognized. In addition, methanotrophy has being recently recognised in *Actinobacteria*, which is reflected by the presence of *pMMO* genes within members of this phylum in the phylogenetic trees of this study. However, their function still needs to be verified by in vitro experiments.

Bibliography

- Bay, S. K., Dong, X., Bradley, J. A., Leung, P. M., Grinter, R., Jirapanjawat, T., Arndt, S. K., Cook, P. L. M., LaRowe, D. E., Nauer, P. A., Chiri, E., & Greening, C. (2021). Trace gas oxidizers are widespread and active members of soil microbial communities. *Nature Microbiology*, 6(2), 246–256. <https://doi.org/10.1038/s41564-020-00811-w>
- Chan, S. I., & Lee, S. J. (2019). *The Biochemistry of Methane Monooxygenases* (pp. 71–120). https://doi.org/10.1007/978-3-030-23261-0_3
- Cui, J., Zhang, M., Chen, L., Zhang, S., Luo, Y., Cao, W., Zhao, J., Wang, L., Jia, Z., & Bao, Z. (2022). Methanotrophs Contribute to Nitrogen Fixation in Emergent Macrophytes. *Frontiers in Microbiology*, 13. <https://doi.org/10.3389/fmicb.2022.851424>
- Culpepper, M. A., & Rosenzweig, A. C. (2012). Architecture and active site of particulate methane monooxygenase. In *Critical Reviews in Biochemistry and Molecular Biology* (Vol. 47, Issue 6, pp. 483–492). <https://doi.org/10.3109/10409238.2012.697865>
- de Assis Costa, O. Y., Meima-Franke, M., & Bodelier, P. L. E. (2021). Complete and Draft Genome Sequences of Aerobic Methanotrophs Isolated from a Riparian Wetland. *Microbiology Resource Announcements*, 10(9). <https://doi.org/10.1128/MRA.01438-20>
- Deutzmann, J. S., Hoppert, M., & Schink, B. (2014). Characterization and phylogeny of a novel methanotroph, *Methyloglobulus morosus* gen. nov., spec. nov. *Systematic and Applied Microbiology*, 37(3), 165–169. <https://doi.org/10.1016/j.syapm.2014.02.001>
- Dimitri Kits, K., Campbell, D. J., Rosana, A. R., & Stein, L. Y. (2015). Diverse electron sources support denitrification under hypoxia in the obligate methanotroph *Methylobacterium album* strain BG8. *Frontiers in Microbiology*, 6(OCT). <https://doi.org/10.3389/fmicb.2015.01072>
- Dunfield, P. F., Yuryev, A., Senin, P., Smirnova, A. V., Stott, M. B., Hou, S., Ly, B., Saw, J. H., Zhou, Z., Ren, Y., Wang, J., Mountain, B. W., Crowe, M. A., Weatherby, T. M., Bodelier, P. L. E., Liesack, W., Feng, L., Wang, L., & Alam, M. (2007). Methane oxidation by an extremely acidophilic bacterium of the phylum Verrucomicrobia. *Nature*, 450(7171), 879–882. <https://doi.org/10.1038/nature06411>
- Guerrero-Cruz, S., Vaksmaa, A., Horn, M. A., Niemann, H., Pijuan, M., & Ho, A. (2021). Methanotrophs: Discoveries, Environmental Relevance, and a Perspective on Current and Future Applications. In *Frontiers in Microbiology* (Vol. 12). Frontiers Media S.A. <https://doi.org/10.3389/fmicb.2021.678057>

- Hadley Wickham. (2016). *ggplot2: Elegant Graphics for Data Analysis* (978-3-319-24277-4). Springer-Verlag New York. <https://ggplot2.tidyverse.org>
- Hadley Wickham, & Jennifer Bryan. (2022). *readxl: Read Excel Files* (R package version 1.4.1). <https://CRAN.R-project.org/package=readxl>
- Hadley Wickham, Romain François, Lionel Henry, & Kirill Müller. (2022). *dplyr: A Grammar of Data Manipulation* (R package version 1.0.10). <https://CRAN.R-project.org/package=dplyr>
- Han, D., Dedysh, S. N., & Liesack, W. (2018). Unusual Genomic Traits Suggest *Methylocystis bryophila* S285 to Be Well Adapted for Life in Peatlands. *Genome Biology and Evolution*, *10*(2), 623–628. <https://doi.org/10.1093/gbe/evy025>
- Hanson, R. S., & Hanson, T. E. (1996). Methanotrophic Bacteria. In *MICROBIOLOGICAL REVIEWS* (Vol. 60, Issue 2). <https://journals.asm.org/journal/mr>
- Im, J., Lee, S. W., Yoon, S., Dispirito, A. A., & Semrau, J. D. (2011). Characterization of a novel facultative *Methylocystis* species capable of growth on methane, acetate and ethanol. *Environmental Microbiology Reports*, *3*(2), 174–181. <https://doi.org/10.1111/j.1758-2229.2010.00204.x>
- Islam, T., Jensen, S., Reigstad, L. J., Larsen, Ø., & Birkeland, N.-K. (2008). *Methane oxidation at 55 o C and pH 2 by a thermoacidophilic bacterium belonging to the Verrucomicrobia phylum.* www.pnas.org/cgi/content/full/
- Kalyaanamoorthy, S., Minh, B. Q., Wong, T. K. F., Von Haeseler, A., & Jermiin, L. S. (2017). ModelFinder: Fast model selection for accurate phylogenetic estimates. *Nature Methods*, *14*(6), 587–589. <https://doi.org/10.1038/nmeth.4285>
- Katoh, K., Rozewicki, J., & Yamada, K. D. (2018). MAFFT online service: Multiple sequence alignment, interactive sequence choice and visualization. *Briefings in Bioinformatics*, *20*(4), 1160–1166. <https://doi.org/10.1093/bib/bbx108>
- Khadka, R., Clothier, L., Wang, L., Lim, C. K., Klotz, M. G., & Dunfield, P. F. (2018). Evolutionary History of Copper Membrane Monooxygenases. *Frontiers in Microbiology*, *9*. <https://doi.org/10.3389/fmicb.2018.02493>
- Kits, K. D., Klotz, M. G., & Stein, L. Y. (2015). Methane oxidation coupled to nitrate reduction under hypoxia by the Gammaproteobacterium *Methylomonas denitrificans*, sp. nov. type strain FJG1. *Environmental Microbiology*, *17*(9), 3219–3232. <https://doi.org/10.1111/1462-2920.12772>

- Knief, C. (2015). Diversity and habitat preferences of cultivated and uncultivated aerobic methanotrophic bacteria evaluated based on pmoA as molecular marker. In *Frontiers in Microbiology* (Vol. 6, Issue DEC). Frontiers Media S.A. <https://doi.org/10.3389/fmicb.2015.01346>
- Kolb, S., & Horn, M. A. (2012). Microbial CH₄ and N₂O consumption in acidic wetlands. *Frontiers in Microbiology*, 3(MAR). <https://doi.org/10.3389/fmicb.2012.00078>
- Koo, C. W., & Rosenzweig, A. C. (2021). Biochemistry of aerobic biological methane oxidation. In *Chemical Society Reviews* (Vol. 50, Issue 5, pp. 3424–3436). Royal Society of Chemistry. <https://doi.org/10.1039/d0cs01291b>
- Koo, C. W., Tucci, F. J., He, Y., & Rosenzweig, A. C. (2022). *Recovery of particulate methane monooxygenase structure and activity in a lipid bilayer*.
- Lee, D.-H., Madhavaraj, L., Han, G. H., Lee, H., Lee, S.-G., & Kim, S. W. (2020). Complete Genome Sequence of *Methylomonas koyamae* LM6, a Potential Aerobic Methanotroph. *Microbiology Resource Announcements*, 9(6). <https://doi.org/10.1128/MRA.01544-19>
- Letunic, I., & Bork, P. (2021). Interactive tree of life (iTOL) v5: An online tool for phylogenetic tree display and annotation. *Nucleic Acids Research*, 49(W1), W293–W296. <https://doi.org/10.1093/nar/gkab301>
- Lieberman, R. L., & Rosenzweig, A. C. (2004). Biological methane oxidation: Regulation, biochemistry, and active site structure of particulate methane monooxygenase. In *Critical Reviews in Biochemistry and Molecular Biology* (Vol. 39, Issue 3, pp. 147–164). <https://doi.org/10.1080/10409230490475507>
- Lieberman, R. L., & Rosenzweig, A. C. (2005). *Crystal structure of a membrane-bound metalloenzyme that catalyses the biological oxidation of methane*. www.nature.com/nature
- Liew, E. F., Tong, D., Coleman, N. V., & Holmes, A. J. (2014). Mutagenesis of the hydrocarbon monooxygenase indicates a metal centre in subunit-C, and not subunit-B, is essential for copper-containing membrane monooxygenase activity. *Microbiology (United Kingdom)*, 160(PART 6), 1267–1277. <https://doi.org/10.1099/mic.0.078584-0>
- Madeira, F., Pearce, M., Tivey, A. R. N., Basutkar, P., Lee, J., Edbali, O., Madhusoodanan, N., Kolesnikov, A., & Lopez, R. (2022). Search and sequence analysis tools services from EMBL-EBI in 2022. *Nucleic Acids Research*, 50(W1), W276–W279. <https://doi.org/10.1093/nar/gkac240>

- Minh, B. Q., Nguyen, M. A. T., & Von Haeseler, A. (2013). Ultrafast approximation for phylogenetic bootstrap. *Molecular Biology and Evolution*, *30*(5), 1188–1195. <https://doi.org/10.1093/molbev/mst024>
- Nguyen, L. T., Schmidt, H. A., Von Haeseler, A., & Minh, B. Q. (2015). IQ-TREE: A fast and effective stochastic algorithm for estimating maximum-likelihood phylogenies. *Molecular Biology and Evolution*, *32*(1), 268–274. <https://doi.org/10.1093/molbev/msu300>
- Op den Camp, H. J. M., Islam, T., Stott, M. B., Harhangi, H. R., Hynes, A., Schouten, S., Jetten, M. S. M., Birkeland, N. K., Pol, A., & Dunfield, P. F. (2009). Environmental, genomic and taxonomic perspectives on methanotrophic Verrucomicrobia. In *Environmental Microbiology Reports* (Vol. 1, Issue 5, pp. 293–306). <https://doi.org/10.1111/j.1758-2229.2009.00022.x>
- Oremland, R. S., & Culbertson, C. W. (1992). Importance of methane-oxidizing bacteria in the methane budget as revealed by the use of a specific inhibitor. *Nature*, *356*(6368), 421–423. <https://doi.org/10.1038/356421a0>
- Peng, S., Lin, X., Thompson, R. L., Xi, Y., Liu, G., Hauglustaine, D., Lan, X., Poulter, B., Ramonet, M., Saunois, M., Yin, Y., Zhang, Z., Zheng, B., & Ciais, P. (2022). Wetland emission and atmospheric sink changes explain methane growth in 2020. *Nature*, *612*(7940), 477–482. <https://doi.org/10.1038/s41586-022-05447-w>
- Philipp Schaubberger, & Alexander Walker. (2022). *openxlsx: Read, Write and Edit xlsx Files* (R package version 4.2.5.1). <https://CRAN.R-project.org/package=openxlsx>
- Pol, A., Heijmans, K., Harhangi, H. R., Tedesco, D., Jetten, M. S. M., & Op den Camp, H. J. M. (2007). Methanotrophy below pH 1 by a new Verrucomicrobia species. *Nature*, *450*(7171), 874–878. <https://doi.org/10.1038/nature06222>
- R Core Team. (2022). *R: A Language and Environment for Statistical Computing*. R Foundation for Statistical Computing. <https://www.R-project.org/>
- Reim, A., Lüke, C., Krause, S., Pratscher, J., & Frenzel, P. (2012). One millimetre makes the difference: High-resolution analysis of methane-oxidizing bacteria and their specific activity at the oxic-anoxic interface in a flooded paddy soil. *ISME Journal*, *6*(11), 2128–2139. <https://doi.org/10.1038/ismej.2012.57>
- Ro, S. Y., Ross, M. O., Deng, Y. W., Batelu, S., Lawton, T. J., Hurley, J. D., Stemmler, T. L., Hoffman, B. M., & Rosenzweig, A. C. (2018). From micelles to bicelles: Effect of the

- membrane on particulate methane monooxygenase activity. *Journal of Biological Chemistry*, 293(27), 10457–10465. <https://doi.org/10.1074/jbc.RA118.003348>
- Sayers, E. W., Bolton, E. E., Brister, J. R., Canese, K., Chan, J., Comeau, D. C., Connor, R., Funk, K., Kelly, C., Kim, S., Madej, T., Marchler-Bauer, A., Lanczycki, C., Lathrop, S., Lu, Z., Thibaud-Nissen, F., Murphy, T., Phan, L., Skripchenko, Y., ... Sherry, S. T. (2022). Database resources of the national center for biotechnology information. *Nucleic Acids Research*, 50(D1), D20–D26. <https://doi.org/10.1093/nar/gkab1112>
- Sharir-Ivry, A., & Xia, Y. (2021). Quantifying evolutionary importance of protein sites: A Tale of two measures. *PLoS Genetics*, 17(4). <https://doi.org/10.1371/journal.pgen.1009476>
- Sojo, V., Dessimoz, C., Pomiankowski, A., & Lane, N. (2016). Membrane Proteins Are Dramatically Less Conserved than Water-Soluble Proteins across the Tree of Life. *Molecular Biology and Evolution*, 33(11), 2874–2884. <https://doi.org/10.1093/molbev/msw164>
- Tavormina, P. L., Orphan, V. J., Kalyuzhnaya, M. G., Jetten, M. S. M., & Klotz, M. G. (2011). A novel family of functional operons encoding methane/ammonia monooxygenase-related proteins in gammaproteobacterial methanotrophs. *Environmental Microbiology Reports*, 3(1), 91–100. <https://doi.org/10.1111/j.1758-2229.2010.00192.x>
- Trifinopoulos, J., Nguyen, L. T., von Haeseler, A., & Minh, B. Q. (2016). W-IQ-TREE: a fast online phylogenetic tool for maximum likelihood analysis. *Nucleic Acids Research*, 44(W1), W232–W235. <https://doi.org/10.1093/NAR/GKW256>
- van Spanning, R. J. M., Guan, Q., Melkonian, C., Gallant, J., Polerecky, L., Flot, J. F., Brandt, B. W., Braster, M., Iturbe Espinoza, P., Aerts, J. W., Meima-Franke, M. M., Piersma, S. R., Bunduc, C. M., Ummels, R., Pain, A., Fleming, E. J., van der Wel, N. N., Gherman, V. D., Sarbu, S. M., ... Bitter, W. (2022). Methanotrophy by a Mycobacterium species that dominates a cave microbial ecosystem. *Nature Microbiology*, 7(12), 2089–2100. <https://doi.org/10.1038/s41564-022-01252-3>
- Vorobev, A., Jagadevan, S., Jain, S., Anantharaman, K., Dick, G. J., Vuilleumier, S., & Semrau, J. D. (2014). Genomic and Transcriptomic Analyses of the Facultative Methanotroph *Methylocystis* sp. Strain SB2 Grown on Methane or Ethanol. *Applied and Environmental Microbiology*, 80(10), 3044–3052. <https://doi.org/10.1128/AEM.00218-14>
- Zheng, Y., Wang, H., Liu, Y., Zhu, B., Li, J., Yang, Y., Qin, W., Chen, L., Wu, X., Chistoserdova, L., & Zhao, F. (2020). Methane-Dependent Mineral Reduction by Aerobic Methanotrophs

under Hypoxia. *Environmental Science and Technology Letters*, 7(8), 606–612.
<https://doi.org/10.1021/acs.estlett.0c00436>

Zhu, Y., Koo, C. W., Cassidy, C. K., Spink, M. C., Ni, T., Zanetti-Domingues, L. C., Bateman, B., Martin-Fernandez, M. L., Shen, J., Sheng, Y., Song, Y., Yang, Z., Rosenzweig, A. C., & Zhang, P. (2022). Structure and activity of particulate methane monooxygenase arrays in methanotrophs. *Nature Communications*, 13(1). <https://doi.org/10.1038/s41467-022-32752-9>